

In uence of external magnetic elds on growth of alloy nanoclusters

M Einax^{1,2}, S Heinrichs¹, P Maass², A Majhofer³ and
W Dieterich¹

¹ Universität Konstanz – Fachbereich Physik, D-78457 Konstanz, Germany

² Technische Universität Ilmenau – Institut für Physik, D-98684 Ilmenau, Germany

³ University of Warsaw – Institute of Experimental Physics, Hoza 69, PL-00681
Warszawa, Poland

E-mail: mario.einax@tu-ilmenau.de

Abstract. Kinetic Monte Carlo simulations are performed to study the influence of external magnetic fields on the growth of magnetic fcc binary alloy nanoclusters with perpendicular magnetic anisotropy. The underlying kinetic model is designed to describe essential structural and magnetic properties of CP_{t_3} -type clusters grown on a weakly interacting substrate through molecular beam epitaxy. The results suggest that perpendicular magnetic anisotropy can be enhanced when the field is applied during growth. For equilibrium bulk systems a significant shift of the onset temperature for $L1_2$ ordering is found, in agreement with predictions from Landau theory. Stronger field induced effects can be expected for magnetic fcc-alloys undergoing $L1_0$ ordering.

PACS numbers: 81.15.Aa, 68.55.-a, 75.30.Gw

Submitted to: J. Phys.: Condens. Matter

1. Introduction

It has recently been shown that CoPt₃ ultrathin films and nanoclusters, grown by molecular beam epitaxy (MBE), display perpendicular magnetic anisotropy (PMA) with potential applications in high density magnetic storage media [1, 2, 3]. Previous simulations of CoPt₃ nanocluster growth on a weakly interacting substrate suggested that PMA originates from the combined effects of Pt surface segregation and cluster shape [4, 5]. As suggested by experiments on Co-Pt multilayer systems [6], out-of-plane CoPt bonds contribute to a magnetic anisotropy energy that tends to align the Co-moments along the bond direction and thus favours PMA. When a perpendicular magnetization is induced by a magnetic field applied during growth, this type of a local magnetic anisotropy energy can be expected to lead to an additional preference of out-of-plane relative to in-plane nearest neighbour Co-Pt pairs. MBE-growth of CoPt₃-clusters in a perpendicular field should therefore improve the formation of PMA in nanoclusters.

In order to demonstrate this latter effect we perform kinetic Monte Carlo simulations of growth within a binary alloy model, supplemented by a magnetic anisotropy energy H_A based on Co-Pt bond contributions. Isotropic magnetic interactions, on the other hand, do not contribute in a significant way to any growth-induced structural anisotropy. Their main effect in growth simulations is a small renormalization of chemical interactions, which can be neglected. However, both types of magnetic interactions in Co-Pt and related fcc-alloys can lead to an intriguing interplay between structural ordering phenomena and magnetism in samples at equilibrium [7]. We confirm this by comparing predictions of Landau theory with equilibrium Monte Carlo simulations.

2. Definition of the model

The model we consider refers to binary fcc-alloys with composition AB_3 . A minimal set of chemical interactions between the atoms is chosen that is consistent with the main processes during structure formation: atomic migration in different local environments, surface segregation of the majority atoms and ordering with $L1_2$ -symmetry. On a semiquantitative level, these features can be reproduced by effective chemical interactions V_{AA} , V_{AB} and V_{BB} acting between nearest neighbour A or B-atoms on an fcc lattice. The linear combinations $I = (V_{AA} + V_{BB} - 2V_{AB})/4$, $h = V_{BB} - V_{AA}$ and $V_0 = (V_{AA} + V_{BB})/2$ determine the bulk ordering temperature $T_0 = 1.83I/k_B$ [8], the degree of surface segregation of one atomic species and the average atomic binding energy, respectively. Following previous work [4], we adapt our model to CoPt₃ (A = Co, B = Pt), where $T_0 \approx 960$ K, and Pt-surface segregation is strong (nearly 100% [9]). Compatible parameters are $I = 1$, $h \approx 4$ and $V_0 \approx 5$, where we have used $k_B T_0 = 1.83 \approx 45$ meV, corresponding to 523 K, as our energy unit. The value for V_0 describes the average binding energy for intermediate coordination numbers experienced by atoms within the growth zone near the cluster surface. The substrate (111) surface

is weakly attractive with a potential $V_s = -5$ that acts on adatoms in the first layer. Compared to a Pt(111) surface with three bonds of typical strength V_0 , this amounts to about 1/3 of the energy of a single Pt-Pt bond.

The elementary processes in our continuous time kinetic Monte Carlo algorithm, which drive the cluster growth, are (i) codeposition of A- and B-atoms with ratio 1:3 and total flux F , (ii) hopping of atoms to vacant nearest neighbour sites, and (iii) direct exchange of unlike nearest neighbour atoms; one of them is an adatom with low coordination (3 to 5) on top of a terrace and the other one a highly coordinated atom (coordination 8 to 10) underneath. Such exchange processes facilitate Pt segregation to the surface, which otherwise becomes kinetically hindered through the incoming flux. In our simulations we choose $F = 3.5$ monolayers per second. As far as possible, other kinetic parameters are adapted from known diffusion data: Jump rates for A and B atoms are of the form $\exp[-(U + \max(0; E))/k_B T]$ where $\nu = 8.3 \cdot 10^{11} \text{ s}^{-1}$ is the attempt frequency, $U = 5$ [10] is the diffusion barrier, and E denotes the energy difference before and after the jump. Direct exchange processes among pairs of unlike atoms are subjected to an increased barrier $U + U_x$ with $U_x = 5$. For more details on that model and on the choice of these parameters we refer to [4].

As explained in the introduction, PMA in CoPt₃-nanoclusters can be related to a structural anisotropy, expressed by the parameter

$$P = (n_o^{\text{CoPt}} - n_k^{\text{CoPt}})/N; \quad (1)$$

which is defined in terms of the difference between numbers of Co-Pt bonds out of plane, n_o^{CoPt} , and in plane, n_k^{CoPt} . N is the total number of atoms in the cluster. The underlying analysis [4] can in particular account for the temperature window where PMA occurs, which lies below the onset of L1₂ ordering. Furthermore, it provides an interpretation of PMA in terms of cluster size and shape, and the degree of Pt-surface segregation. The associated magnetic model assumes a local crystalline anisotropy energy H_A , that involves only Co-moments as its dominant part. Within a bond picture, each Co-atom experiences an anisotropy energy that is a sum over Co-Pt bond contributions

$$A (\sum_j \mathbf{r}_{ij}^2) \quad (2)$$

Here \mathbf{r}_{ij} is a bond vector connecting the Co-atom with one of its nearest neighbour Pt atoms, and $A = 225$ eV is a parameter deduced from the interfacial part of the measured magnetic anisotropy of Co-Pt multilayers [6]. We remark that these measurements also appear to justify the bond model implied by (2), when two different interfacial orientations are compared. For (111) interfaces the anisotropy energy per surface area is found about twice as large as for the (100) orientation. Considering the different angles of bonds to the surface and the different packings, equation (2) indeed can reproduce this difference with one consistent value for A . Since $A > 0$, spin alignment along a Co-Pt bond is favoured. Certainly, A is small relative to the chemical interactions V_{AA} , V_{AB} and V_{BB} as well as I and h . Hence, in the absence of a magnetic field it is justified in a first approximation to neglect (2) in simulating growth,

but to include it a posteriori in order to relate a given cluster structure to its magnetic properties.

3. Growth in external fields

However, when an external magnetic field is applied, we show here that inclusion of the magnetic anisotropy energy (2) in the growth process itself leads to a small but notable change in the clusters' short range order such that PMA gets enhanced [11]. To demonstrate this, we apply a strong field B_s perpendicular to the substrate that drives the magnetization towards saturation. Components in (2) are then aligned along the [111] direction, which introduces an asymmetry in the probabilities for jumps that form or break CoPt-bonds. For in-plane bonds, (2) gives no contribution, whereas the energy of an out-of-plane CoPt bond is changed from V_{AB} to $V_{AB}^0 = V_{AB} - \frac{2}{3}A$ in the fcc lattice geometry.

Clearly, the expected magnetic field effects on growth are small in view of the smallness of the magnetic anisotropy parameter A in (2). To obtain reliable results for the change in the structural anisotropy parameter P with and without the field, we have carried out simulations including several much larger parameters A up to $A = 1$. Note that the energy unit chosen (see above) implies that the physical value $A = 250$ eV corresponds to $A = 5 \cdot 10^3$. Results for those different artificial A -values will be used in turn to extract the physical change of P by interpolation.

From this analysis we first show results for the dependence $P = P(N; A)$ on cluster size N , see figure 1. All data sets referring to different A exhibit an approximate linearity in $N^{-1/3}$,

$$P(N; A) \approx p_s(A) N^{-1/3}; \quad (3)$$

Concerning the N -dependence, this confirms that the structural anisotropy essentially is a surface effect. The figure includes the case $A = 0$, represented by open symbols. This data formally corresponds to zero magnetic field, because for $B = 0$ at the temperatures considered the components are oriented randomly so that (2) gives no contribution to P . The important observation is that $P(N; A)$ for fixed N significantly increases with A . Figure 2 explicitly shows that the behaviour of the coefficient $p_s(A)$ obtained from fits according to (3), appears to be consistent with a linear A -dependence. Assuming linearity even in the limit $A \rightarrow 0$, we obtain $(p_s(A) - p_s(0)) \approx p_s(0) \cdot 3 \cdot 10^2$ for the physical value $A = 5 \cdot 10^3$.

This result immediately translates to the magnetic field-dependence of the structural part of the total magnetic anisotropy energy E_s , which is proportional to NP . Using (3), we can write

$$E_s = K_s(B) N^{2/3}; \quad (4)$$

z Fits of data in figure 1 by straight lines and extrapolation to $N^{-1/3} \rightarrow 0$ yield in addition a non-zero bulk contribution to P which, however, is negligibly small in comparison with P -values for clusters with $N = 10^3$ atoms.

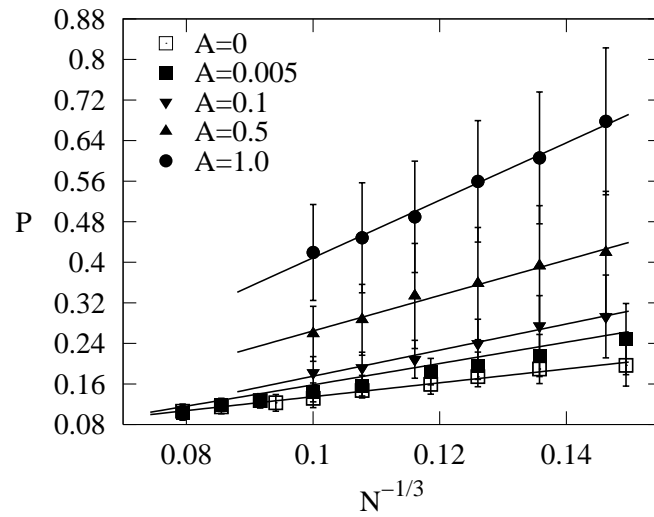


Figure 1. Simulated structural anisotropy parameter P depending on cluster size N in the presence of the saturation field B_s at temperature $k_B T = 1.2$ ($T \approx 630\text{K}$). Averages are performed over 20 clusters. Full lines display linearity in $N^{-1/3}$. Open symbols are equivalent to the case of zero magnetic field.

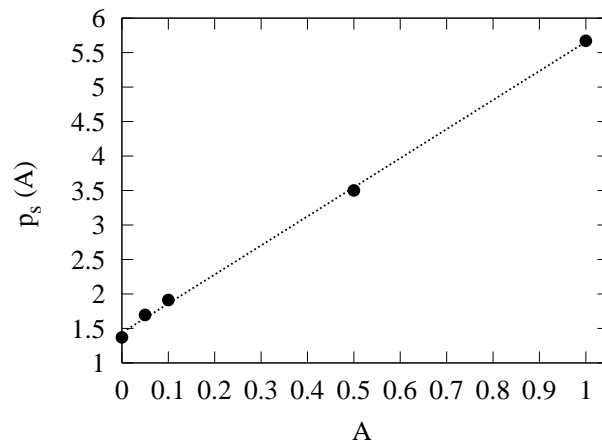


Figure 2. Coefficient $p_s(A)$ determining the structural anisotropy versus the magnetic anisotropy constant A at $T = 1.2$. Data points result from the slopes of Figure 1 including the case $A = 0.05$. Dotted line: linear fit.

again with the relative change $(K_s(B_s) - K_s(0))/K_s(0) \approx 3 \cdot 10^2$. Thus, our main result is that the surface anisotropy constant K_s in (4) increases by about 3% when a perpendicular field of the strength of the saturation field B_s is switched on. Near $T \approx 1$ ($T \approx 523\text{K}$), where the anisotropy develops its maximum [11], we obtain analogous results (not shown).

4. Interplay of structural and magnetic order in the bulk

So far we have shown that in the presence of a strong perpendicular magnetic field the anisotropy energy H_A notably affects the frozen-in structure of growing nanoclusters and thus improves PMA. Based on Landau theory, we now study effects of external magnetic fields on the equilibrium structure of bulk systems or homogeneous films. Effects of this type are known in principle but have been explored only for few specific materials [2]–[13]. For CoPt₃, quantitative calculations have been performed in the past within the cluster variation method in the tetrahedron approximation [14]. Landau theory, which we use here allows us to incorporate the magnetic anisotropy in a simple manner and helps clarifying the interrelation between different effects.

For the free energy f per Co-atom in CoPt₃ in the presence of an external field B we propose the form

$$f = f_S + f_M + f_{\text{int}}(M, B); \quad (5)$$

where $M = (M_1; M_2; M_3)$ is the average magnetic moment per CoPt₃-unit. The first term in (5) denotes the structural free energy that describes L1₂-ordering without magnetic contributions [15],

$$f_S = \sum_{i=1}^3 \frac{r(T)}{2} X_i^2 + \frac{v}{4} X_i^4 + \frac{u}{4} \sum_{i=1}^3 X_i^3 + w_{123}; \quad (6)$$

The structural order parameter components X_i , $i = 1; 2; 3$, describe amplitudes for layering along one of the cubic axes of the fcc-lattice such that CoPt-layers and Pt-layers alternate. Superposition of these layer structures in all three directions yields the L1₂-structure. As usual, we set $r(T) = r_0(T - T_{\text{sp}})$; $r_0 > 0$, $u > 0$, $0 < v < u$ and $w > 0$, where T_{sp} denotes the spinodal temperature. The associated ordering temperature T_0 is determined by $r(T_0) = (2-9)w^2 = (3u + v)$.

The second term in (5) is the isotropic magnetic free energy, with the behaviour

$$f_M(M) = \frac{b(T)}{2} M^2; \quad (7)$$

as $M \rightarrow 0$, where $b(T) = b_0(T - T_C)$ and T_C denotes the Curie-temperature of a disordered alloy. Finally the third term in (5), f_{int} describes the coupling between structural and magnetic order. Retaining only the lowest-order terms allowed by symmetry, we write

$$f_{\text{int}} = \frac{C_1}{2} \sum_{i=1}^3 X_i^3 M^2 + \frac{C_2}{2} \sum_{i=1}^3 X_i^3 M^2; \quad (8)$$

For later purposes we define the Landau coefficients such that they become dimensionless, with $j = j_{\text{max}} = 1$ for perfect structural order. Expressions (5)–(8) imply far-reaching interdependencies between structural and magnetic properties. Combination with simple mean-field arguments allows us to make order-of-magnitude predictions which can be tested experimentally.

First, collecting terms in (5) which are quadratic in M , we find that in a state magnetized parallel to the [111] direction, both the spinodal and the transition temperature for $L1_2$ -ordering are shifted by an amount $T_{sp}(M) = T_{sp}' - T_0(M) = T_0 - T_0(M)$ with

$$T_0(M) = (3c_1 + c_2)M^2 = 3r_0: \quad (9)$$

To determine the coefficients in (9) we note that the same combination $3c_1 + c_2$ enters the difference in Curie temperatures between disordered and ordered samples,

$$T_C(m_{ax}) - T_C = (3c_1 + c_2) = b_0: \quad (10)$$

This relation is immediately obtained from (5) by requiring the terms quadratic in M to vanish. For the ordered samples we have set $j = j'_{m_{ax}}$, because the discontinuity ρ_0 in χ at T_0 is large and Curie temperatures are considerably lower than $T_0' \approx 960$ K. Within the same consideration the inverse magnetic susceptibility χ^{-1} develops a discontinuity at the order transition at T_0 of magnitude $(3c_1 + c_2) \frac{2}{\rho_0}$. Experimentally, $T_C(m_{ax}) \approx 400$ K, while $T_C = 150$ K [14]. The reason for an increased Curie temperature in quenched, disordered samples is the increased number of Co-Co direct exchange couplings relative to the ordered state. This temperature shift already allows a rough estimate of (9). Suppose, for example, the magnetic field is strong enough to drive the magnetic moment M to values near its saturation value M_s . Using mean field arguments, we expect that both k_B and $b_0 M_s^2 = k_B$ are of order unity. Therefore the two expressions (10) and (9) should be of similar magnitude. In other words, for very strong magnetic fields $B \parallel [111]$ equation (9) predicts a lowering of T_0 by about $T_{0,m_{ax}} \approx 10^2$ K in CoPt_3 .

A further effect is worth mentioning. When the orientation of the external field is changed from [111] to [001] and $c_2 < 0$, the disordered phase develops an instability towards formation of a layered structure with $\rho_1 = \rho_2 = 0$ and $\rho_3 \neq 0$, i.e. with $L1_0$ symmetry. The corresponding transition point is increased relative to the spinodal temperature for [111] field orientation, $T_{sp}(M)$, by an amount $(2-3)j_2j$, but will exceed $T_0(M)$ only if j_2j is sufficiently large. Otherwise this layered structure cannot form because the conventional ordering transition at $T_0(M)$ will set in before. In CoPt_3 anisotropic magnetic interactions determining c_2 are weak (see below) so that this effect is unlikely to be observable.

At this point let us attempt to explicitly relate the parameters c_1 and c_2 to a specific magnetic model. For that purpose we adopt a phenomenological spin-Hamiltonian $H_M = H_{ex} + H_A$ pertaining to CoPt_3 alloys. As its main contribution we assume classical Heisenberg-type isotropic exchange interactions H_{ex} within nearest-neighbour Co-Co and Co-Pt pairs. This simplified form seems sufficient as we are dealing only with the energetics of homogeneously magnetized states. The respective magnetic energies for Co-Co and Co-Pt pairs with parallel spins are JM_s^2 and $J'M_s^2$, respectively. In xPt-moments have been shown to depend on the actual atomic environment [14] but this effect is neglected here.

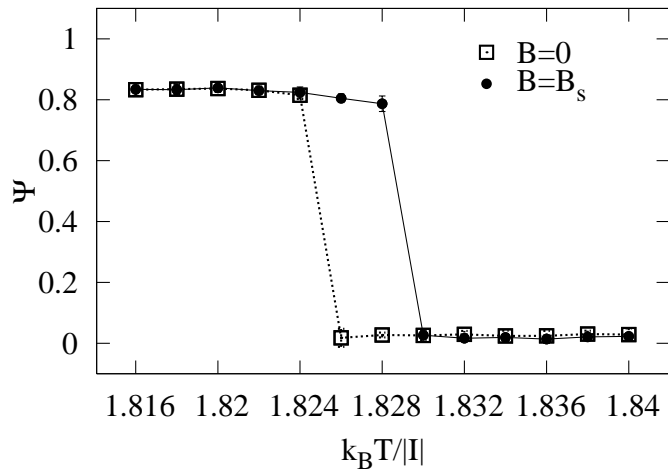


Figure 3. Simulated $L1_2$ order parameter (η) for a bulk system at equilibrium as a function of temperature. Averages were performed over 6 realizations. Among the magnetic interactions only the anisotropy H_A has been included in the simulations. The upward shift of the ordering temperature $T_0(B) = T_0' + 2K$ is clearly recognizable.

In addition, an anisotropy H_A connected with Co-Pt bonds, see (2), is included. Within first order perturbation theory the change in free energy due to H_M is given by an average of H_M over an unperturbed ensemble specified by the . Mean-field calculations then yield

$$c_1 = J - 2J^2; \quad c_2 = -2A - M_s^2: \quad (11)$$

In order to test the validity of the Landau approach based on the coupling (8) between structural and magnetic order and its prediction (9), we first focus on the anisotropy energy H_A (ignoring H_{ex}) and perform Monte Carlo simulations of the lattice model described before, but now under equilibrium conditions. The simulation box contains 43200 atoms and is subjected to periodic boundary conditions in all three directions. Equilibrated configurations are generated by allowing any pair of unlike atoms to exchange positions. In figure 3 the structural order parameter is plotted versus temperature, and indeed shows an increased transition temperature in the fully magnetized state in comparison to the zero field case. We have again used $A = 225$ eV, see above, which gives an increase of T_0 by 2K. This increase favourably agrees with (9) when we set $c_1 = 0$, see (11), and $r_0 = k_B^{-1}$. These results show that with realistic parameters for the microscopic anisotropy energy a measurable shift in the ordering temperature is observed. The physical reason for the increase of T_0 in figure 3 is that through the presence of H_A the six nearest neighbour sites of a Co-atom with bond vectors not orthogonal to $[111]$ become preferentially occupied by Pt-atoms during the equilibration process, thus favouring the ordered structure. Basically this is the same mechanism that yields an increased structural anisotropy parameter P discussed before. Figure 3, therefore, provides additional evidence, that H_A affects the ordering transition.

When exchange interactions are included, equation (9) predicts a much larger downward shift in T_0 , which we can estimate now in a more quantitative manner. From [14] and known Co- and Pt- moments we obtain $JM_s^2 \approx 140 \text{ K}$ and $J^0M_s^2 \approx 25 \text{ K}$, while A is much smaller. Thus $(3c_1 + c_2)M_s^2 = 3 \approx 90 \text{ K}$, in agreement with the order of magnitude estimate of (9) given before, which was based on the comparison with measured Curie temperatures.

Again, the corresponding change in T_0 according to (9) can be compared with predictions from numerical computation. However, within a lattice model with nearest-neighbour chemical and isotropic exchange interactions, extra simulations for this problem actually are not needed when we note that in a fully magnetized sample the effect of H_{ex} is simply equivalent to modified chemical interactions

$$V_{AA}^0 = V_{AA} - JM_s^2; \quad V_{BB}^0 = V_{BB}; \quad V_{AB}^0 = V_{AB} - JM_s^2: \quad (12)$$

Since the ordering transition temperature satisfies $k_B T_0 \approx 1.83(V_{AA} + V_{BB} - 2V_{AB})/4$, we find, using (12), $k_B T_0(M_s) \approx 1.83(J - 2J^0)M_s^2/4$. Because of (11) and $|j_2| < c_1$ this is consistent with (9) and establishes a semi-quantitative estimate $T_0(M_s) \approx 41 \text{ K}$. Clearly, since the exchange terms JM_s^2 and $J^0M_s^2$ in (12) are relatively small, we could neglect them in our previous discussion of structural anisotropy.

Experimentally, for CoPt_3 it is probably very difficult to induce a sufficiently strong magnetization near T_0 such that the shift T_0 / M^2 becomes measurable. The situation is more favourable for $L1_0$ -ordering of $\text{Co}_x\text{Pt}_{1-x}$ alloys near $x = 0.5$, where the Curie temperature is closer to the ordering temperature T_0 and even intersects with T_0 on the Co-rich side in the phase diagram. A similar situation occurs for Ni-rich $\text{Ni}_x\text{Pt}_{1-x}$ alloys [7]. For $L1_0$ -ordering the structural part of the free energy f_s is again based on (6), however, with a change in sign in w at $x = 1/2$, v sufficiently negative and additional stabilizing higher order terms [16]. Elastic energy contributions due to the tetragonal distortion in the $L1_0$ phase are thereby neglected. Coupling between structural order parameters and the magnetization can again be represented by equation (8). Considering magnetic fields $B \parallel [001]$ we now obtain $T_{\text{sp}}(M) \approx T_0(M) = (c_1 + c_2)M^2 = T_0$ and $T_C(\text{max}) = (c_1 + c_2) = T_0$ instead of (9) and (10), with a measured value of about 10^2 K for the latter temperature shift. Using similar arguments as before, both temperature shifts $T_{\text{sp}}(M_s)$ and $T_C(\text{max})$ are expected to be of the same order.

5. Conclusions and outlook

Effects of external magnetic fields on both the far-from-equilibrium MBE growth of magnetic fcc alloys and their bulk structural phase behaviour at equilibrium have been studied. The statistical model we employed pertains to binary alloys of the CoPt_3 type and $L1_2$ -ordering. KMC simulations are supplemented by equilibrium considerations based on Landau theory. Using realistic parameters for CoPt_3 our main aim was to explore the influence of the local crystalline magnetic anisotropy energy, modelled

by a bond Hamiltonian H_A , on the structural properties of alloy nanoclusters, when a strong magnetic field is applied during growth. Such an effect, although small in CoPt_3 , appears to be general and indeed leads to a notable enhancement of the clusters structural anisotropy and the associated PMA. Experimentally, in order to induce a large magnetization, the substrate temperature should fall below the Curie temperature of disordered samples but at the same time remain in the known temperature window where PMA occurs.

More favorable conditions for studying these effects experimentally should exist for alloys like CoPt or FePt [17] undergoing $L1_0$ -ordering, if clusters could be grown along the c -axis. As known from thin film measurements [8], the magnetic anisotropy in those alloys is a bulk property connected with alternating Co(Fe) - and Pt -rich layers caused by the $L1_0$ structural order. Hence, under growth conditions where $L1_0$ -ordering is suppressed, one can expect a substantially larger field-induced PMA.

Acknowledgments

We thank M. Albrecht and G. Schatz for fruitful discussions. This work has been supported by the Deutsche Forschungsgemeinschaft DFG (SFB 513).

References

- [1] Albrecht M, Maier A, Treubel F, Maret M, Poinot P and Schatz G 2001 *Europhys. Lett.* 56 884
- [2] Albrecht M, Maret M, Maier A, Treubel F, Riedlinger B, Mazur U, Schatz G and Anders S 2002 *J. Appl. Phys.* 91 8153
- [3] Shapiro L, Rooney P W, Tran M Q, Hellman F, Ring K M, Kavanagh K L, Rellinghaus B and Weller D 1999 *Phys. Rev. B* 60 12826
- [4] Heinrichs S, Dieterich W and Maass P 2006 *Europhys. Lett.* 75 167
- [5] Heinrichs S, Dieterich W and Maass P 2006 *Epitaxial growth of binary alloy nanostructures* Preprint cond-mat/0607284
- [6] Johnson M T, Blomen P J H, den Broeder F J A and de Vries J J 1996 *Rep. Prog. Phys.* 59 1409
- [7] Cadeville M C and Moran-Lopez J L 1987 *Phys. Rep.* 153 331
- [8] Binder K 1980 *Phys. Rev. Lett.* 45 811
- [9] Gauthier Y, Baudoing-Savois R, Bugnard J M, Bardi U and Atré A 1992 *Surf. Sci.* 276 1
- [10] Bott M, Hohage M, Morgenstem M, Michely T and Comsa G 1996 *Phys. Rev. Lett.* 76 1304
- [11] Einax M, Heinrichs S, Maass P, Majhofer A, and Dieterich W *Proc. E-MRS 2006 Spring Meeting (Nice)*, *Material Science and Engineering: C*, in press
- [12] Chikazumi S and Graham C D 1999 *Physics of Ferromagnetism* 2nd edition (Oxford: Oxford University Press)
- [13] Dang M Z and Rancourt D G 1996 *Phys. Rev. B* 53 2291
- [14] Sanchez J M, Moran-Lopez J L, Leroux C and Cadeville M C 1989 *J. Phys. C: Condens. Matter* 1 491
- [15] Lai Z W 1990 *Phys. Rev. B* 41 9239
- [16] Tanoglu G B, Braun R J, Cahn J W and McFadden G B 2003 *Interfaces and free boundaries* 5 275
- [17] Massalski T, 1996 *Binary alloy phase diagrams vol2* (Ohio: ASM International)
- [18] Iwata S, Yamashita S and Tsunashima S 1997 *IEEE Transactions on Magnetics*, 33 3670